Contribution from the Department of Chemistry,
The University of North Carolina, Chapel Hill, North Carolina 27514

The Oxo-Bridged Ions $[(NH_3)_5RuORu(NH_3)_5]^{n+}$ (n = 4, 5)

JOHN A. BAUMANN and THOMAS J. MEYER*

Received May 2, 1979

The oxo-bridged dimer $[(NH_3)_5RuORu(NH_3)_5]^{4+}$ and the analogous 5+, mixed-valence ion have been prepared and characterized. The properties of the ions are consistent with strong electronic coupling between the ruthenium ions through the oxo ligand, and the mixed-valence ion, which is formally a Ru(III)–Ru(IV) case, appears to be delocalized.

Introduction

A number of chemically well-defined dimeric and oligomeric complexes of ruthenium are known where the link between metal sites is a μ-oxo bridging ligand. The systems known include dimers like $[Cl_5RuORuCl_5]^{4-}$,[1] and $[(bpy)_2ClRuORuCl(bpy)_2]^{2+}$ (bpy is 2,2′-bipyridine),[2] oligomers like "ruthenium-red", $[(NH_3)_5RuORu(NH_3)_4ORu(NH_3)_5]^{6+}$,[3] and clusters like $[Ru_3O(CH_3CO_2)_6(py)_3]^+$ (py is pyridine).[4] One reason for an interest in such systems is that the oxo group can support strong electronic interactions between the metal sites,[2] which can, in turn, lead to an extensive, reversible redox chemistry.[2,4] In more general terms, strong electronic coupling can lead to new chemical systems where the chemical and physical properties at the metal sites are significantly modified compared to related monomers. In this context, oxo-bridged dimers and oligomers are potential sources of new materials that may have their own distinct chemical and physical properties.

The ion $[Ru(NH_3)_5(H_2O)]^{2+}$ and the related 2+ hexaammine ion are known to be air sensitive in water. They react with oxygen to give the nearly colorless Ru(III) ions $Ru(NH_3)_5H_2O^{3+}$ and $Ru(NH_3)_6^{3+}$.[5] By contrast, the ion $[Ru(NH_3)_5(S)]^{2+}$ (S = acetone), which has proven useful as a synthetic intermediate,[6-9] is also air sensitive, but exposure of the ion to oxygen in acetone results in a dramatic color change from the characteristic deep orange of the acetone complex to an intense red. The details of the reaction with O_2 will be discussed in more detail in a later paper, but the point of interest here is the fact that the major product of the reaction is the dimer $[(NH_3)_5RuORu(NH_3)_5]^{4+}$. The dimer and its properties are of value because the existence of the ion fills in a gap for the simple dimeric analogue of ruthenium-red, and its properties are of interest in comparison with other dimers.

Experimental Section

Measurements. Ultraviolet and visible spectra were recorded by using Cary Models 14 and 17 and Bausch and Lomb Model 210 spectrophotometers. Infrared spectra were recorded on a Perkin-Elmer 421 spectrophotometer in KBr pellets, at room temperature. Electrochemical measurements made were vs. the saturated sodium chloride calomel electrode (SSCE) at 25 ± 2 °C and are uncorrected for junction potential effects. The measurements were made by using a PAR Model 173 potentiostat for potential control with a PAR Model 175 universal programmer as a sweep generator for voltammetric experiments. Values of n, where n is the number of moles of electrons transferred per mole of complex in an exhaustive electrolysis at constant potential, were calculated after measuring the total area under current vs. time curves for complete electrolysis. Reactions were judged to be complete when the current had fallen below 1% of its initial value. Electrochemical reversibility was determined by cyclic voltammetry, on the basis of the ratio of cathodic to anodic peak currents (i_c/i_a) and the potential separation of the oxidation and reduction peaks (ΔE_p) for each electron-transfer process. All voltammetric measurements were carried out at platinum electrodes. The solutions were deaerated by a stream of dry argon or nitrogen when potential scans or electrolyses were carried out at negative potentials.

Solution conductivity measurements were made in acetone and acetonitrile at 25 °C by using an Industrial Instruments, Inc., Model RC-16B1 conductivity bridge. Cell constants for the platinized platinum electrode conductivity cell were determined at 25 °C from measurements of the conductivity of 0.0100 M aqueous solutions of potassium chloride.[10] For spectrophotometric titrations, solutions of Br_2 in CH_3CN were standardized by using $\epsilon = 183 \pm 4$ M^{-1} cm^{-1} at 395 nm.[7] The titrations were carried out by adding aliquots of oxidant (Br_2) to solutions of the complex and monitoring the changes in absorbance at 503 and 342 nm.

Materials. Tetra-*n*-butylammonium hexafluorophosphate (TBAH) was recrystallized three times from hot ethanol–water mixtures and vacuum dried at 70 °C for 10 h. Acetonitrile (MCB Spectrograde) was dried over Davidson 4-Å molecular sieves for electrochemical measurements and used without drying for spectral measurements. Water was deionized and then distilled from alkaline permanganate. All other solvents (reagent grade) were used without further purification. Argon was purified by passing it through a heated column of activated Catalyst R3-11 (Chemical Dynamics Corp.) and then through drying tubes containing Drierite. Elemental analyses were carried out by Galbraith Laboratories, Knoxville, Tenn., and Integral Microanalytical Laboratories, Raleigh, N.C.

Preparations. $[Ru(NH_3)_5Cl]Cl_2$ (1). The salt was prepared according to the procedure of Vogt et al.[11] and recrystallized from hot (ca. 80–90 °C) 0.1 M hydrochloric acid.

$[(NH_3)_5Ru(OH_2)](PF_6)_2 \cdot H_2O$ (2a). The $[(NH_3)_5Ru(OH_2)]^{2+}$ ion was generated essentially by the method of Harrison et al.,[12] slightly modified by Callahan[6] and appearing in several papers.[7-9] The only further modification was the use of a Schlenk-type apparatus. A solution containing $[(NH_3)_5RuCl]Cl_2$ was reduced over Zn–Hg amalgam in the upper portion of the apparatus and filtered into a saturated aqueous solution of NH_4PF_6, which caused the precipitation of the desired complex as the PF_6^- salt. Argon was passed into the bottom chamber, through the frit, and out the top during the reduction step. The Ar flow was reversed to effect filtration of the solution of $[Ru(NH_3)_5(H_2O)]^{2+}$ from the Zn–Hg amalgam.

$[(NH_3)_5Ru(S)](PF_6)_2$ (2b) (S = Acetone). The aquo ligand was replaced by acetone by dissolving a portion of the pentaammine–aquo complex, **2a**, in deaerated acetone. After being stirred for 1 min, the solution was transferred through a needle to a flask of stirred, deaerated

(1) J. D. Dunitz and L. E. Orgel, *J. Chem. Soc.*, 2594 (1953).
(2) T. R. Weaver, T. J. Meyer, S. Adeyemi, G. M. Brown, R. P. Eckberg, W. E. Hatfield, E. C. Johnson, R. W. Murray, and D. Untereker, *J. Am. Chem. Soc.*, **97**, 3039 (1975).
(3) J. E. Earley and T. Fealey, *Inorg. Chem.*, **12**, 323 (1973).
(4) (a) A. Spencer and G. Wilkinson, *J. Chem. Soc., Dalton Trans.*, 1570 (1973); (b) J. A. Baumann, D. J. Salmon, S. T. Wilson, T. J. Meyer, and W. E. Hatfield, *Inorg. Chem.*, **17**, 3342 (1978).
(5) J. R. Pladziewicz, J. A. Broomhead, T. J. Meyer, and H. Taube, *Inorg. Chem.*, **12**, 639 (1973).
(6) R. W. Callahan, Ph.D. Dissertation, The University of North Carolina, Chapel Hill, N.C., 1975, p 115.
(7) R. W. Callahan, G. M. Brown, and T. J. Meyer, *Inorg. Chem.*, **14**, 1443 (1975).
(8) R. W. Callahan, G. M. Brown, and T. J. Meyer, *J. Am. Chem. Soc.*, **96**, 7829 (1974).
(9) B. P. Sullivan, J. A. Baumann, T. J. Meyer, D. J. Salmon, H. Lehmann, and A. Ludi, *J. Am. Chem. Soc.*, **99**, 7368 (1977).
(10) H. H. Willard, L. L. Merritt, and J. A. Dean, "Instrumental Methods of Analysis", 4th ed., Van Nostrand, New York, 1965, p 720.
(11) L. H. Vogt, Jr., J. L. Katz, and S. E. Wiberly, *Inorg. Chem.*, **4**, 1157 (1965).
(12) D. E. Harrison, H. Taube, and E. Weissberger, *Science*, **159**, 320 (1968).

0020-1669/80/1319-0345$01.00/0

diethyl ether, which caused precipitation of the PF_6^- salt. After collection and drying in a vacuum, the complex was immediately used in method 1 for the preparation of the oxo-bridged dimer.

$[(NH_3)_5RuORu(NH_3)_5](PF_6)_4$ (3a). Method 1. In a typical preparation involving O_2 as oxidant, 195 mg of **2b**, $[(NH_3)_5Ru(S)](PF_6)_2$ (0.365 mmol), was placed in the top portion of a Schlenk-type apparatus. Diethyl ether (100 mL) was placed in the bottom section. The joints were fitted with serum caps, and the whole apparatus was flushed with a flow of argon, from the bottom section to the top. After 15 min, 10 mL of acetone (freshly distilled and also deaerated with argon) was transferred into the top portion via a needle from a separate acetone reservoir. Oxygen was then passed intermittently through the acetone solution via the bottom half through the frit. After a few minutes, the solution became slightly pink, and the O_2 flow was then maintained continuously for 15 min, the color becoming quite dark red. A vigorous flow of argon then replaced the O_2 in order to reduce the volume slightly ($\simeq$20%). The direction of flow was then reversed (top to bottom), filtering the solution and leaving behind a dark red solid. This solid was washed by injecting Et_2O into the upper portion several times, the argon flow eventually drying the solid. The dried solid was then recovered, placed in a vial, and dried in a vacuum desiccator; yield 111 mg (51% based on analysis). The filtrate precipitated a solid upon mixing with the Et_2O in the bottom flask. It was collected and dried. Its spectrum included absorption bands at λ_{max} = 542 and 342 nm. Analysis of the dimer prepared by this method shows that acetone coprecipitates with the complex. Anal. Calcd for **3a**, $[(NH_3)_5RuORu(NH_3)_5](PF_6)_4 \cdot 4CH_3COCH_3$: C, 12.00; H, 4.53; N, 11.67. Found: C, 11.81; H, 4.34; N, 11.58.

Method 2. A small amount (ca. 10 mg) of $[N(n\text{-}C_4H_9)_4](PF_6)$(TBAH) was dissolved in 15 mL of freshly distilled acetone and the mixture deaerated with argon. In a separate 25-mL flask, 200.54 mg of **2**, $[Ru(NH_3)_5(OH_2)](PF_6)_4 \cdot 4H_2O$ (0.405 mmol), and 32.4 mg of $LiClO_4$ (0.306 mmol) were combined, along with a stir bar. The flask was fit with a serum cap and deaerated 15 min, after which 10 mL of the TBAH–acetone mixture was transferred to the flask containing the solids via a needle. The solution was covered and stirred under a blanket of argon for 15 min. An equal volume of diethyl ether was injected into the flask, and the mixture was stirred for 1 min. It was then filtered to collect the resulting precipitate, which was washed well with methylene chloride (to remove excess TBAH) and Et_2O and dried. Anal. Calcd for **3b**, $[(NH_3)_5RuORu(NH_3)_5](PF_6)_4$: C, 0.00; H, 3.12; N, 14.47. Found: C, <0.03; H, 3.25; N, 14.46. (The original filtrate yielded a precipitate upon addition of further amounts of Et_2O. It was collected and also showed λ_{max} = 542 and 342 nm.)

$[(NH_3)_5RuORu(NH_3)_5]Br_4$ (3c). The bromide salt was prepared from the PF_6^- salt by dissolving the latter in a minimum amount of acetone and adding excess tetra-*n*-butylammonium bromide. On addition of methylene chloride, the bromide salt of the complex precipitated. It was collected and washed well with acetone, methylene chloride, and Et_2O. Finally it was air-dried. Anal. Calcd for **3c**, $[(NH_3)_5RuORu(NH_3)_5]Br_4 \cdot {}^1/_2CH_2Cl_2$: C, 1.59; H, 4.13; N, 18.51; Br, 42.25. Found: C, 1.47; H, 4.22; N, 18.87; Br, 39.70.

$[(NH_3)_5RuORu(NH_3)_5]Br_5$ (4a). The 4+ complex was oxidized to the 5+ ion by dissolving 100 mg of the PF_6^- salt (**3a** or **3b**) in a minimum of CH_3CN. Excess Br_2 was diluted in CH_3CN and the mixture added dropwise to the solution containing the 4+ ion. The color immediately disappeared, and a precipitate formed. An equal volume of methylene chloride was added to complete the precipitation, and the solution was filtered to collect the solid. Depending upon the purity of the starting 4+ dimer, the color of the solid was brown or green (see Results). The collected solid was washed with CH_3CN, CH_2Cl_2, and then Et_2O and air-dried; yield 65 mg (94% based on analysis). Anal. Calcd for **4a**, $[(NH_3)_5RuORu(NH_3)_5]Br_5 \cdot CH_3CN$: C, 2.90; H, 4.01; N, 18.54; Br, 48.19. Found: C, 2.64; H, 3.78; N, 17.54; Br, 44.14.

$[(NH_3)_5RuORu(NH_3)_5]Cl_5$ (4b). The Br^- complex was placed on a column of Sephadex SP-C25-120 ion-exchange resin (2.5-cm diameter × 4-cm height column), eluted with 0.4 M HCl, and precipitated by adding acetone. Other species observed on the column were $[(NH_3)_5RuCl]^{2+}$, which eluted with 0.2 M HCl, and "ruthenium-brown", which eluted with 0.8 M HCl. When elution was done with NaCl instead of HCl, 2.0 M NaCl was necessary to elute the green complex. On standing several weeks, NaCl solutions yielded small dark green crystals among the larger NaCl crystals. The two could be physically separated to obtain the green crystals. Anal. Calcd for **4b**, $[(NH_3)_5RuORu(NH_3)_5]Cl_5$: C, 0.0; H, 5.34; N, 24.76; Cl, 31.33. Found: C, <0.04; H, 5.19; N, 24.09; Cl, 31.44.

$[(ND_3)_5RuORu(ND_3)_5]Cl_4$ (5). Deuterated samples were needed for IR spectra and were freshly prepared by dissolving a portion of the PF_6^- salt (**3a** or **3b**) in deaerated D_2O and stirring the solution under argon for 1.5 h. A small amount of LiCl was added to the solution followed by a large volume of previously deaerated acetone, which precipitated the Cl^- salt. The complex was air-dried and immediately pressed into a KBr pellet.

$[(ND_3)_5RuORu(ND_3)_5]Br_5$ (6). Another portion of the 4+ complex as the PF_6^- salt (**3a** or **3b**) was dissolved in a minimum of deaerated acetonitrile. D_2O was added to the solution, and it was stirred for 45 min. Bromine was added to the solution which oxidized the complex. Addition of methylene chloride precipitated the Br^- salt, which was collected, air-dried and immediately pressed into a KBr pellet.

Results

Synthesis. In dry acetone, $[(NH_3)_5Ru(S)]^{2+}$ (S = acetone) undergoes a rapid reaction with oxygen to give a red solution containing the 4+ dimer (eq 1). The stoichiometry in eq 1

$$4[(NH_3)_5Ru(S)]^{2+} + O_2 \rightarrow 2[(NH_3)_5RuORu(NH_3)_5]^{4+} + 4S \quad (1)$$

was determined by a spectrophotometric titration, the details of which will be described in a later paper as will the oxidation using ClO_4^- described in method 2 in the Experimental Section. For the titration, the acetone complex used was prepared by method 1 in the Experimental Section.

In the preparations, the acetone was freshly distilled in an attempt to eliminate water because water apparently causes complications in the O_2 oxidations. The reaction between $[(NH_3)_5Ru(S)]^{2+}$ and O_2 is complicated by the formation of Ru-red (λ_{max} at 542 nm in acetone) which occurs on a slower time scale. If trace water is present, the dimer is oxidized further to the "mixed-valence" 5+ ion, $[(NH_3)_5RuORu(NH_3)_5]^{5+}$ (λ_{max} = 342 nm). These two contaminants are always present and appear in the acetone filtrates after isolation of the dimer (see Experimental Section). The mixed-valence dimer can be prepared in bulk by oxidizing the 4+ dimer with Br_2 (eq 2).

$$[(NH_3)_5RuORu(NH_3)_5]^{4+} + {}^1/_2Br_2 \rightarrow [(NH_3)_5RuORu(NH_3)_5]^{5+} + Br^- \quad (2)$$

When pure, $[Ru_2O(NH_3)_{10}]^{4+}$ in acetonitrile is stable for 0.5–1 h as shown by spectral studies. However, for impure samples, especially where there are not noticeable Ru(II) impurities present, decomposition occurs in reactions which are as yet undefined. The 5+ complex is stable for long periods of time in acidic or neutral aqueous solutions as well as in acetonitrile.

Characterization of the 4+ Dimer. The results of a number of experiments support the formulation of the red salt obtained from the O_2 oxidation reaction as the oxo-bridged dimer $[(NH_3)_5RuORu(NH_3)_5]^{4+}$. The stoichiometry of the reaction with O_2 has been mentioned. In addition, chemical oxidation of $[(NH_3)_5RuORu(NH_3)_5]^{4+}$ occurs with a 0.5:2 Br_2:Ru ratio as shown by spectrophotometric titrations,[7,8] which give $[(NH_3)_5RuORu(NH_3)_5]^{5+}$ quantitatively as can be seen in Figure 1. The oxidation can also be carried out electrochemically in which case one electron is lost per two ruthenium, as shown by spectral and cyclic voltammetry experiments (vide infra). The oxidation experiments show that there must be an even number of ruthenium sites in the complex.

Feltham and Hayter[13] have shown that plots of the equivalent conductivity, Λ_e, vs. the square root of the equivalent concentration, $C_e^{1/2}$, are linear with slopes which depend upon

(13) R. D. Feltham and R. G. Hayter, *J. Chem. Soc.*, 4587 (1964).

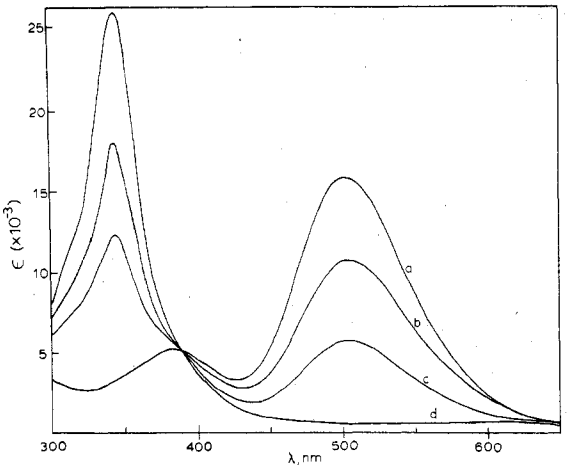

Figure 1. Spectrophotometric titration of $[(NH_3)_5RuORu(NH_3)_5]^{4+}$ with Br_2 in acetonitrile: (a) unititrated compound; (b) 0.17 mol of Br_2/mol of dimer; (c) 0.33 mol of Br_2/mol of dimer; (d) 0.50 mol of Br_2/mol of dimer.

Table I. Solution Conductivity Data for the Oxo-Bridged Dimer and Reference Complexes as PF_6^- Salts in Acetonitrile at 25 °C

compd	Λ_0[a]	slope[a]
$[Ru(bpy)_3](PF_6)_2$	193	663
$\{[Ru(bpy)_2(py)]_2(4,4'\text{-bpy})\}(PF_6)_4$	364	2967
$[(NH_3)_5RuORu(NH_3)_5](PF_6)_4$	344	3309

[a] Determined from plots of Λ_e vs. $C_e^{1/2}$.[13]

Scheme I

$$RuORu^{6+} \xleftarrow{+e^-} RuORu^{5+} \underset{-e^-}{\overset{+e^-}{\rightleftharpoons}} RuORu^{4+} \xrightarrow{+e^-} RuORu^{3+}$$

(+1.67 V) (+0.32 V) (−1.98 V)

the electrolyte type. Λ_0 can be obtained by extrapolation of a plot of Λ_e vs. $C_e^{1/2}$ to infinite dilution. It is clear from the data in Table I that the conductivity data in acetonitrile are consistent with the PF_6^- salt of the dimer being the 4:1 electrolyte $[(NH_3)_5RuORu(NH_3)_5](PF_6)_4$.

Spectral and Redox Properties. In cyclic voltammetry experiments on $[(NH_3)_5RuORu(NH_3)_5](PF_6)_4$ in 0.1 M TBAH–acetonitrile, a single, chemically reversible wave appears at $E_{1/2}$ = 0.32 V for the $[(NH_3)_5RuORu(NH_3)_5]^{4+/5+}$ couple. Coulometry for oxidation of the 4+ to the 5+ ion occurs with $n \approx 1$, and upon reduction back to the 4+ ion, n is also approximately 1, illustrating the chemical reversibility of the couple. The electrochemistry is quasi-reversible at a scan rate of 200 mV/s, with a peak splitting of 80 mV. In 0.1 M TBAH–acetone, $E_{1/2}$ = 0.25 V with ΔE_p = 90 mV at 500 mV/s. In 0.1 M HCl in water, $E_{1/2}$ = −0.175 V with ΔE_p = 60 mV at 200 mV/s.

In addition to the reversible 5+/4+ couple, two other waves are observable in deaerated acetonitrile. One is an irreversible oxidation at $E_{p,a}$ = 1.67 V (no well-defined reduction wave), and the other is an irreversible reduction at $E_{p,c}$ = −1.98 V (with no well-defined oxidation wave). The electrochemical behavior in acetonitrile is summarized in Scheme I.

In Figure 2, UV–visible spectra are shown for the 4+ dimer in acetonitrile as the PF_6^- salt and for the 5+ dimer in water as the Cl^- salt. The λ_{max} values and extinction coefficients are listed in Table II. The data for the 4+ dimer are calculated by assuming a sample composition of $[(NH_3)_5RuORu(NH_3)_5](PF_6)_4 \cdot 4CH_3COCH_3$, on the basis of elemental analysis data for the sample used in the measurement.

The low-energy bands at 503 and 386 nm in the 4+ dimer are very reminiscent of the intense low-energy transitions in other oxo-bridged ruthenium dimers: $[(bpy)_2ClRuORuCl(bpy)_2]^{2+}$, λ_{max} = 672 nm (ϵ = 17 900);[2] $[Cl_5RuORuCl_5]^{4-}$, λ_{max} = 500 nm,[1] and higher oligomers $[(NH_3)_5RuORu(NH_3)_4ORu(NH_3)_5]^{6+}$, λ_{max} = 532 nm (in H_2O) (ϵ = 69 000);[3] $[Ru_3O(OAc)_6L_3]^+$, λ_{max} = 692 nm (ϵ = 5800, L = py).[4] Upon oxidation, the lower energy transition moves to higher energy and becomes more intense. In other complexes, similar shifts on oxidation are observed (e.g., for $[(bpy)_2ClRuORuCl(bpy)_2]^{3+}$, λ_{max} = 400 nm (ϵ = 19 700))[2] but the intensity does not always increase (e.g., for $[(NH_3)_5RuORu(NH_3)_4ORu(NH_3)_5]^{7+}$, λ_{max} = 465 nm (ϵ = 43 800)). In addition to the intense band at 342 nm and the weaker band at 255 nm in the 5+ dimer, there is a very weak, low-energy transition at 617 nm (ϵ = 271), which gives the complex its green color.

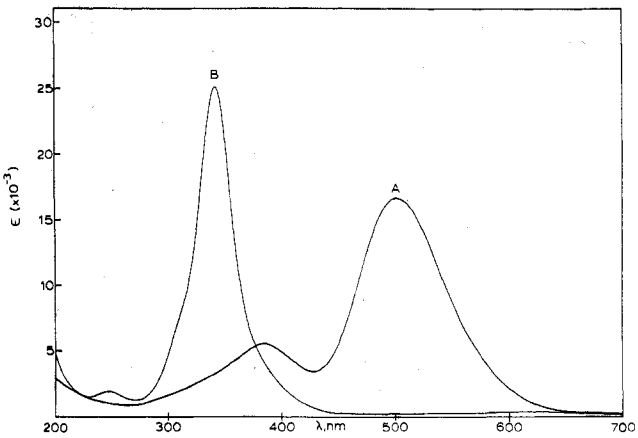

Figure 2. UV–visible spectra for the 4+ and 5+ dimers $[(NH_3)_5RuORu(NH_3)_5]^{n+}$ from 700 to 200 nm: (A) the 4+ dimer as its PF_6^- salt in CH_3CN; (B) the 5+ dimer as its Cl^- salt in H_2O.

Table II. UV–Visible Spectral Data for the Dimers $[(NH_3)_5RuORu(NH_3)_5]^{n+}$ (n = 4, 5)

compd	λ_{max}, nm	ϵ_{max}, M^{-1} cm^{-1}
$[(NH_3)_5RuORu(NH_3)_5]^{4+}$ [a]	503	16230
	386	5430
$[(NH_3)_5RuORu(NH_3)_5]^{5+}$ [b]	616	271
	342	25280
	255	2100

[a] In CH_3CN, by use of the salt $[(NH_3)_5RuORu(NH_3)_5](PF_6)_4 \cdot 4CH_3COCH_3$. [b] In H_2O, by use of the salt $[(NH_3)_5RuORu(NH_3)_5]Cl_5$.

Infrared Spectra. Several authors[14–16] have commented on the characteristic vibrational spectra of oxo-bridged metal complexes. For linear M–O–M species, an infrared-active, asymmetric stretch is found in the range 800–900 cm^{-1}. Bending of the M–O–M linkage results in a lowering of the asymmetric stretching frequency to the 700–800-cm^{-1} range. Bending can also make the corresponding symmetric stretching mode at about 500 cm^{-1} infrared active. Attempts were made to identify characteristic M–O–M stretching frequencies in the infrared spectra of the 4+ and 5+ dimers.

The data for the complexes are summarized in Table III. The 4+ complex was converted from the PF_6^- salt to a bromide salt specifically to be able to clear the 800–900-cm^{-1} region of the strong PF_6^- vibrational bands.[6,17] There are two remaining bands in the 4+ dimer in the region of interest, at 788 and 744 cm^{-1}. In the 5+ dimer, similar bands occur at 812 and 786 cm^{-1}.

(14) D. J. Hewkin and W. P. Griffith, *J. Chem. Soc. A*, 472 (1966).
(15) R. N. Wing and K. P. Callahan, *Inorg. Chem.*, **8**, 871 (1969).
(16) I. San Filippo, Jr., R. L. Graysen, and H. L. Sniadoch, *Inorg. Chem.*, **15**, 269 (1976).
(17) J. A. Baumann, Ph.D. Dissertation, The University of North Carolina, Chapel Hill, N.C., 1978, Chapters 2 and 3.

Table III. IR Data from 2600 to 600 cm^{-1} for $[(NH_3)_5RuORu(NH_3)_5]^{n+}$ and $[(ND_3)_5RuORu(ND_3)_5]^{n+}$ (n = 4, 5) as Chloride or Bromide Salts in KBr

$[Ru_2O(NH_3)_{10}]^{5+}$ [a]	$[Ru_2O(ND_3)_{10}]^{4+}$ [a]	$[Ru_2O(NH_3)_{10}]^{5+}$ [a]	$[Ru_2O(ND_3)_{10}]^{5+}$ [a]	assignt [b]
	2526 m		2422 s	ν(ND)
	2430 sh			
	2386 m		2288 s	ν(ND)
	2352 sh			
1616 m	1625 m	1618 m	1622	$\delta(NH_3)_{deg}$(?)
	1580 sh			
1450 bd, w	1422 bd, w	1550 sh, bd	1450 bd, w	?
		1340 w	1150 bd, w	?
1316 sh				
1286 sh	1187 m			
1272 m	1180 m	1308 m	1102 m	$\delta(NH_3)_{sym}$
1254 m	1170 m	1298 m	1072 s	
1106 m	1047 m			?
788 m		812 m		$\rho(NH_3)$
744 m	747 s	786 sh, w	782 w	M-O-M

[a] bd = broad, m = medium, s = sharp, sh = shoulder, w = weak. [b] Based on assignments from ref 18.

Table IV. Ruthenium $3d_{5/2}$ Binding Energies (eV)[a]

$[(NH_3)_5RuORu(NH_3)_5]Br_4$	280.2
$[(NH_3)_5RuORu(NH_3)_5]Br_5$	282.0
$[(bpy)_2ClRuORuCl(bpy)_2](PF_6)_2$ [b]	280.5
$[(bpy)_2ClRuORuCl(bpy)_2](PF_6)_3$ [b]	282.3

[a] Values referenced to the C 1s peak at 284.4 eV. [b] Data from ref 2.

Creutz[18] has identified the bands that appear in this region for the dimers $[(NH_3)_5Ru(pyr)Ru(NH_3)_5]^{n+}$ (n = 4–6; pyr is pyrazine) as an ammonia rocking frequency ($\rho(NH_3)$) whose energy is dependent upon oxidation state. For example, for n = 4 and X = Br^-, ν = 750 cm^{-1}, while for n = 6 and X = ClO_4^-, ν = 820 and 760 cm^{-1}; apparently for Ru(III) complexes, more than one band can appear. To help identify the bands in the 4+/5+ dimers, we deuterated both complexes (see Experimental Section) in order to shift the ammine bands to low energies. Data for the deuterated complexes also appear in Table III.

After deuteration, only one band remains in the relevant region for both complexes, at ν = 747 cm^{-1} for the 4+ dimer and ν = 782 cm^{-1} for the 5+ dimer. The other bands in the nondeuterated complexes are surely the assigned $\rho(NH_3)$ bands which have been shifted upon deuteration to frequencies below 600 cm^{-1}.

Other ammine bands are also shifted to lower energies upon deuteration. Most striking are the symmetric N–H deformations which appear in the 3200–3300-cm^{-1} region in the NH_3 complexes and which shift to the 2350–2500-cm^{-1} region. The symmetric ammonia deformations ($\delta(NH_3)_{sym}$) which occur from 1250 to 1320 cm^{-1} shift to the 1070–1190-cm^{-1} region. The bands at about 1620 cm^{-1}, assigned by Creutz[18] as the degenerate ammonia deformation ($\delta(NH_3)_{deg}$), do not move upon deuteration, which is not unexpected given the nature of the normal mode. There are some weaker bands (broad shoulders) at slightly lower energies (around 1450 cm^{-1}) which seem to be affected by deuteration but which are not well-defined.

ESCA Spectra. X-ray photoelectron spectral data were taken in the range 270–290 eV with a Du Pont 650 B electron spectrometer using Mg Kα X radiation. Binding energies for the Ru $3d_{5/2}$ levels of the 4+ and 5+ dimers (as Br^- salts) are reported in Table IV and are referenced to the C 1s peak assigned a value of 284.4 eV.[19] Included in Table IV are values for the oxo-bridged dimers $[(bpy)_2ClRuORuCl(bpy)_2]^{n+}$ (n = 2, 3).[2]

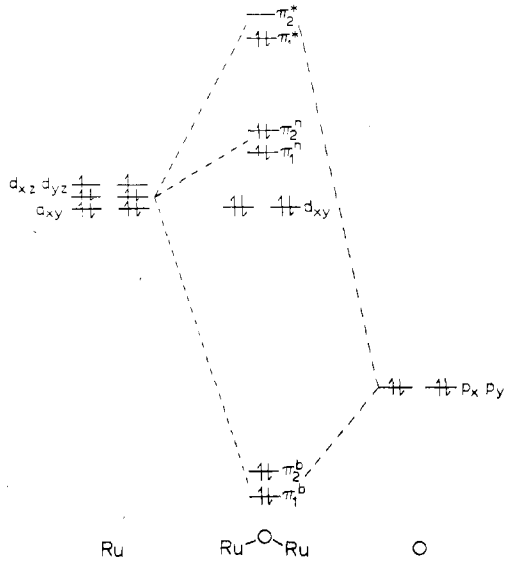

Figure 3. Molecular orbital scheme for a bent Ru–O–Ru system (from ref 2 and 3).

The binding energies for the oxo-bridged ammine complexes are quite close to those for the bipyridine complexes. The observation of a single Ru $d_{5/2}$ peak in the mixed-valence 5+ dimer indicates that the two ruthenium centers are electronically equivalent, or nearly equivalent, and it appears that the Ru sites are strongly coupled.[20]

Magnetic Data. Although not yet completely characterized, the magnetic behavior of the 4+ dimer appears to parallel that of the oxo-bridged bipyridine complexes.[2] At room temperature, the complex exhibits a moment of approximately 1.5 μ_B/ruthenium, a value less than that expected for one unpaired electron per ruthenium. At 18.4 K, the moment falls to 0.38 μ_B/Ru. For the complex $[(bpy)_2(NO_2)RuORu(NO_2)(bpy)_2](PF_6)_2$, the moment at room temperature is 1.84 μ_B/Ru, while at 77.1 K, μ_{eff} = 0.80 μ_B/Ru.

Discussion

Figure 3 is a schematic MO diagram of the type first suggested by Dunitz and Orgel for the oxo-bridged $[Cl_5RuORuCl_5]^{4-}$ ion.[1] The same scheme appears to apply to the ions $[(bpy)_2XRuORuX(bpy)_2]^{2+}$ (X = Cl, NO_2) except that, as shown, the lower symmetry leads to a nondegeneracy of all levels. A lower symmetry is imposed by the unsymmetrical nature of the ligands, but a more important factor

(18) Carol Creutz, Ph.D. Dissertation, Stanford University, 1970, pp 84–6.
(19) P. H. Citrin, *J. Am. Chem. Soc.*, **95**, 6472 (1973).
(20) N. S. Hush, *Chem. Phys.*, **10**, 361 (1975).

in determining the magnitude of the splitting may be the bent Ru–O–Ru structure as shown crystallographically in $[(bpy)_2(NO_2)RuORu(NO_2)(bpy)_2](PF_6)_2$.[21]

The available evidence suggests that a similar diagram is appropriate for $[(NH_3)_5RuORu(NH_3)_5]^{n+}$ and that the electronic structure and redox properties are best thought of in terms of delocalized MO's arising from Ru–O–Ru mixing. The highest, unfilled levels are largely Ru $d\pi^*$ antibonding in character. A lifting of the degeneracy of the π^* levels by Ru–O–Ru bonding is assumed in $[Ru_2O(NH_3)_{10}]^{4+}$ as it was for the bpy complexes. With a bent geometry the degeneracy is lifted, and the oxygen orbitals involved in the orbital mixing are sp hybrids which are probably largely p in character as shown in the diagram.

The splitting of the levels is consistent with a diamagnetic singlet ground state ($^2\pi_1^*$), which is indicated by the small magnetic moment at low temperature. The residual magnetism at low temperature and its increase to a much higher value at room temperature are consistent with the thermal population of the triplet excited state ($^1\pi_1^{*1}\pi_2^*$). In the case of the dimer $[(bpy)_2(NO_2)RuORu(NO_2)(bpy)_2](PF_6)_2$, the temperature dependence of the magnetic susceptibility was fit to the Bleaney–Bowers equation (eq 3).[22] In eq 3, $2J$ is the

$$\chi_M = \frac{Ng^2B^2}{3kT}[1 + \tfrac{1}{3}\exp(-2J/kT)]^{-1} \qquad (3)$$

energy separation between the singlet ground state and the triplet excited state, χ_M is the molar susceptibility calculated per metal ion, and the other constants have their usual meaning. A linear least-squares fit of the data yielded a value of -173 cm^{-1} for $2J$.[2] The data for the 4+ dimer suggest that a similar pattern of levels exists and that the separation between levels is of the same order of magnitude.

In the MO scheme (Figure 3) the highest filled and unfilled levels are largely Ru $d\pi^*$ in character, and the redox behavior is carried by delocalized levels. This is consistent with oxidation of the 4+ ion to the "mixed-valence" $RuORu^{5+}$ complex. In the 5+ ion, the one unpaired electron should be delocalized over both metals, and the ESCA experiment shows a single Ru $3d_{5/2}$ binding energy at 282.0 eV consistent with equivalent Ru sites.

Structures of the Dimers. Although the 4+ and 5+ dimers are almost certainly oxo-bridged dimers, the details of their molecular structures are unknown, and in particular, it is not known whether they are linear or bent. Examples of linear systems are known as in the Ru(IV)–Ru(IV) dimer $(Cl_5RuORuCl_5)^{4-}$,[1] and the dimer $[(bpy)_2(NO_2)RuORu(NO_2)(bpy)_2]^{2+}$ is known to be bent.[21]

The infrared data are ambiguous with respect to the question of structure. While a band remains in the M–O–M regions for both complexes upon deuteration, assignments of the band as the linear M–O–M asymmetrc band or the bent M–O–M symmetric band cannot be made with certainty. For example, the band at 782 cm^{-1} for the deuterated 5+ dimer (Table III) may be the asymmetric band for the linear structure which is shifted to lower energy than the asymmetric band in $[Cl_5RuORuCl_5]^{4-}$ (at 888 cm^{-1})[16] because an additional electron has been added to the $d\pi^*$ orbitals (Figure 3). The antibonding character of the $d\pi^*$ levels means that occupation by an additional electron should lower the M–O–M frequency and that occupation by a second electron to give a Ru(III) ion as in $[(ND_3)_5RuORu(ND_3)_5]^{4+}$ should cause a further lowering (747 cm^{-1} observed).

However, the bands could equally well be assigned to asymmetric stretching frequencies for a bent dimeric structure,[16] and there is reason to believe that at least the 4+ dimer is bent. The interpretation of the magnetic data in terms of Figure 3 is consistent with a bent structure, and related complexes of Ru and of iron, e.g., $[(TPP)_2Fe]_2O$ (TPP is tetraphenylporphine),[23] where there are sterically far more demanding ligands, are known to be bent. The 5+ ion is an odd-electron system which from the Jahn–Teller theorem will be distorted if the loss in electronic energy when orbital degeneracies are removed is sufficient to compensate for any gain in vibrational energy in the new structure. A reasonable distortion would be a bending along the Ru–O–Ru axis.

UV–Visible Spectra. UV–visible spectra are frequently characteristic for oxo-bridged complexes.[2-4] The origins of the transitions are readily accounted for by using a delocalized molecular orbital description like that in Figure 4. Clark et al.[24] have pointed out that in linear systems (i.e., $[Cl_5RuORuCl_5]^{4-}$), the $\pi^* \leftarrow \pi^b$ transition is not allowed by symmetry, and the low-energy absorption bands observed for linear oxo-bridged dimers are thought to be $\pi^* \leftarrow \pi^n$ transitions, which are allowed. The $\pi^* \leftarrow d_{xy}$ transition is also allowed and, if the relative ordering of levels in the MO scheme in Figure 4 is correct, should occur at higher energies than the $\pi^* \leftarrow \pi^n$ transitions.

There are several possible assignments for the absorption bands observed for the 4+ and 5+ decaammine dimers. On the assumption that the 4+ dimer is bent, the bands at 503 nm (19 900 cm^{-1}) and 306 nm (25 900 cm^{-1}) may be $\pi^* \leftarrow \pi^n$ and $\pi^* \leftarrow d_{xy}$ transitions, but the implied splitting between the π^n and d_{xy} levels seems rather large. More reasonable assignments for the bands may be that the lower energy band arises from an overlap of a series of transitions to the π^* level from π_1^n, π_2^n, and d_{xy} and the higher energy band from $\pi^* \leftarrow \pi^b$ transition which is allowed in the lower symmetry of a bent structure.

Absorption bands appear for the 5+ dimer at 342 (29.2×10^3 cm^{-1}) and 255 nm (39.2×10^3 cm^{-1}). If the assignments for the 4+ dimer are correct, the band at 342 nm may be assignable to the $\pi^* \leftarrow \pi^n$ and $\pi^* \leftarrow d_{xy}$ transitions shifted to higher energies upon oxidation. There is a noticeable high-energy shoulder on the band at 310 nm.

The low-energy band in the 5+ dimer (617 nm) is weak ($\epsilon = 271$ M^{-1} cm^{-1}). The band is most probably a transition from the half-filled $d\pi^*$ orbital to an e_g σ^* orbital. The latter orbitals are predominantly localized on the individual metal sites but may have some delocalized character due to mixing via the oxygen. Such a transition as described here is not much different from a d–d transition, except for the molecular orbital character of the π^* orbitals. d–d transitions are not often found in even simple ruthenium complexes because the t_{2g}–e_g^* energy separations are so high that the transitions are usually buried beneath other, stronger transitions such as charge-transfer bands. In the 5+ dimer, no other bands occur at low energies, while the unusually high energy of the π^* orbitals results in a low $e_g^* \leftarrow \pi^*$ transition energy.

Comparisons with Other Systems. The 4+ and 5+ decaammine dimers are interesting additions to the known oxo-bridged complexes of ruthenium. For all members of this class of compounds, the same general conclusions have been reached.[1-4] Strong electronic coupling between the metal sites through the intervening oxo ligand leads to new systems whose chemical and physical properties are noticeably modified compared to those of related monomers. New, intense elec-

(21) D. W. Phelps, E. M. Kahn, and D. J. Hodgson, *Inorg. Chem.*, **14**, 2486 (1975).
(22) B. Bleaney and K. Bowers, *Proc. R. Soc. London, Ser. A*, **214**, 451 (1952).
(23) A. B. Hoffman, D. M. Collins, U. W. Day, E. B. Fleischer, T. S. Srivastava, and J. L. Hood, *J. Am. Chem. Soc.*, **94**, 3620 (1972).
(24) R. J. Clark, M. L. Franks, and P. C. Turtle, *J. Am. Chem. Soc.*, **99**, 2473 (1977).

tronic absorption bands appear as one consequence of the electronic coupling. The gain or loss of electrons involves delocalized molecular levels and the formation of delocalized mixed-valence ions.

The 4+ and 5+ ions are the dimeric analogues of ruthenium-red, $[(NH_3)_5RuORu(NH_3)_4RuORu(NH_3)_5]^{6+}$, and ruthenium-brown, $[(NH_3)_5RuORu(NH_3)_4ORu(NH_3)_5]^{7+}$, which themselves may be members of a chemically accessible set of higher oligomers.[25] Although it is not our intention to make detailed comparisons in this paper, it is interesting to note that the effect of increased number of interacting ions is what would might have been expected intuitively. For example, for the lowest energy, intense absorption band, λ_{max} is at 503 nm for the 4+ dimer and at 532 nm for Ru-red.

Another comparison of interest is between the decaammine dimers and the analogous bpy dimers like $[(bpy)_2ClRuORuCl(bpy)_2]^{3+/2+}$ where the Ru–O–Ru interaction is presumably somewhat modified by changes in the nonbridging ligands.[2] From the comparison of the [3,3] dimers $[(NH_3)_5RuORu(NH_3)_5]^{4+}$ and $[(bpy)_2ClRuORuCl(bpy)_2]^{2+}$, both apparently have similar ground states, probably similar structures, and stable, delocalized [3,4] ions. The low-energy optical spectra of both the [3,3] and [3,4] ions are dominated by what appear to be $\pi^* \leftarrow \pi^n$, d_{xy} transitions which are at significantly lower energies for the bpy dimers: 672 nm for $[(bpy)_2ClRuOCl(bpy)_2]^{2+}$ and 470 nm for $[(bpy)_2ClRuORuCl(bpy)_2]^{3+}$. In the context of the MO diagram in Figure 3, the smaller π^*–$d\pi^n$ energy gap suggested by the spectral results also suggests that the extent of Ru–O–Ru electronic coupling is less for the bpy dimers. Also by use of Figure 3, comparative values of redox potentials suggest that the π_1^*, π_2^* levels are at higher energy for the decaammine system, making it easier to oxidize. In both cases, the potentials for oxidation to a high formal oxidation state [Ru(IV)] are remarkably low, apparently due to the extensive destabilization of the highest, largely $d\pi$(Ru) levels due to the Ru–O–Ru interaction. The relatively low potential for reduction of $[(bpy)_2ClRuORuCl(bpy)_2]^{2+}$ may have its origin in strong mixing by configurational interaction between the π^* levels and low-lying, vacant π^* levels on the 2,2′-bipyridyl ligands.

Acknowledgment. Acknowledgments are made to the Army Research Office—Durham (Grant No. DAAG29-76-G-0135) for support of this research.

Registry No. **1**, 18532-87-1; **2a**, 34843-18-0; **2b**, 72049-59-3; **3a**, 72049-57-1; **3c**, 72049-55-9; **4a**, 72186-96-0; **4b**, 72186-95-9; **5**, 72049-54-8; **6**, 72186-94-8.

(25) J. A. Baumann, Ph.D. Dissertation, The University of North Carolina, Chapel Hill, N.C., 1978.

Contribution from the Miami Valley Laboratories, The Procter & Gamble Company, Cincinnati, Ohio 45247

Structural Investigations of Calcium-Binding Molecules. 5. Structure Analysis of a Calcium Salt of Benzenehexacarboxylic Acid (Mellitic Acid), $Ca_2C_{12}H_2O_{12}\cdot 9H_2O$

VERNON A. UCHTMAN* and RONALD J. JANDACEK

Received July 17, 1979

The crystal and molecular structure of dicalcium dihydrogen mellitate nonahydrate was determined by three-dimensional X-ray crystal structure analysis using a combination of direct and heavy-atom methods. $Ca_2C_{12}H_2O_{12}\cdot 9H_2O$ crystallizes in orthorhombic space group $P2_12_12_1$ with $a = 6.825(2)$ Å, $b = 16.615(5)$ Å, and $c = 18.857(6)$ Å and four formula units per unit cell. Block-diagonal least-squares refinement using automated diffractometer-collected data resulted in $R_1 = 7.8\%$ and $R_2 = 4.8\%$. The crystal structure consists of an extended network of calcium ion coordinated mellitate acid anions and water molecules linked by a complex hydrogen-bonding network. The mellitate acid anions have the two acid hydrogen atoms on meta-related carboxyl groups and are linked together by strong (2.465 and 2.530 Å) intermolecular hydrogen bonds. The two independent calcium ions are seven- and eight-coordinate, respectively. The primary binding between the calcium ions and the mellitate ion is through the formation of four-membered chelate rings utilizing bidentate carboxylate groups. Equilibrium binding constants between Ca^{2+} and mellitate^{6-} were determined via potentiometric titrations utilizing a calcium ion selective electrode. The data could be best fit by the following concentration constants (25 °C, ionic strength 0.1 M KCl): $K_{11} = (3.05 \pm 0.15) \times 10^3$ (mol·L)$^{-1}$ and $K_{21} = (0.37 \pm 0.03) \times 10^3$ (mol·L)$^{-1}$.

Introduction

A continuing program of structural investigations of calcium salts has sought to determine characteristics of calcium binding and to relate solid-state properties (as revealed by single-crystal X-ray analysis) of calcium complexes to behavior in aqueous solution. In part, the purpose of these studies is derived from the considerable interest in finding environmentally innocuous alternatives to polyphosphates for calcium sequestration. Polycarboxylic acids such as benzenehexacarboxylic acid (or salts thereof), otherwise known as mellitic acid, have been suggested[1] as such phosphorus-free nitrogen-free alternatives. Recent studies have also indicated that in an ionized state mellitic acid can function as a crystal growth inhibitor in calcium phosphate precipitation reactions.[2] A determination of the crystal and molecular structure of a calcium salt of mellitic acid was thus viewed as important in the calcium coordination studies being undertaken in our laboratories. Other studies discussed below have indicated a rather stable aqueous complexation between Ca^{2+} and the mellitate anion, $C_{12}O_{12}^{6-}$. It is of particular interest to us to know how Ca^{2+} might bind to a polycarboxylate ligand which does not have the capability for five- or six-membered chelate ring formation (which is traditionally implicated in stable complex formation).

Previously the crystal structure of the parent mellitic acid was reported by Darlow.[3] Also, a recent report on the ionization of polycarboxylic acids, including mellitic acid, has appeared.[4] To our knowledge, there has been only one other

(1) Japanese Patent No. 4709984; Great Britian Patent No. 1317076.

(2) M. D. Francis, C. L. Slough, W. W. Briner and R. P. Oertel, *Calcif. Tissue Res.*, **23**, 53 (1977).

(3) S. F. Darlow, *Acta Crystallogr.*, **14**, 159 (1961).

0020-1669/80/1319-0350$01.00/0